Supplementary Information

Spontaneous helix formation in polar smectic phase

Ewa Gorecka[1], Magdalena Majewska[1], Ladislav Fekete[2], Jakub Karcz[3] Julia Żukowska[3], Jakub Herman[3] Przemysław Kula[3], Damian Pociecha[1*]

[1] Faculty of Chemistry, Warsaw University, Warsaw, Poland
[2] Institute of Physics, Academy of Sciences of Czech Republic, Prague, Czech Republic
[3] Faculty of Advanced Technology and Chemistry, Military University of Technology, Warsaw, Poland

Experimental methods:

Calorimetric studies: For differential scanning calorimetry (DSC) studies, a TA Q200 calorimeter was used, calibrated using indium and zinc standards. Heating and cooling rates were 5-20 K min^{-1}, samples were kept in a nitrogen atmosphere. The transition temperatures and associated thermal effects were extracted from the heating traces.

X-ray diffraction: X-ray diffraction (XRD) studies in broad diffraction angle range were performed with Bruker GADDS system equipped with micro-focus type X-ray tube with Cu anode, and Vantec 2000 area detector. Samples were prepared in the form of small drops placed on a heated surface, their temperature was controlled with a modified Linkam heating stage. For small angle diffraction experiments Bruker Nanostar system was used (micro-focus type X-ray tube with Cu anode, MRI TCPU-H heating stage, Vantec 2000 area detector). Samples were prepared in thin-walled glass capillaries, with 1.5 mm diameter.

Microscopic Studies: Optical textures of LC phases were studied using a Zeiss Axio Imager A2m polarized light microscope, equipped with a Linkam TMS 92 heating stage. Samples were prepared in commercial cells (AWAT) of various thicknesses (1.5–20 µm) with ITO electrodes and surfactant layers for planar or homeotropic alignment, in the case of planar cells either parallel or antiparallel rubbing on both surfaces was applied. Cells for in-plane switching were provided by prof. O. Lavrentovich group at Kent State University.

Optical birefringence: Optical Birefringence was measured with a setup based on a photoelastic modulator (PEM-90, Hinds) working at the base frequency f=50 kHz. As a light source, a halogen lamp (Hamamatsu LC8) equipped with a narrow bandpass filter (532±3 nm) was used. Samples were prepared in glass cells with a thickness of 1.5 µm, having surfactant layers for planar anchoring condition, and parallel rubbing assuring uniform alignment of the optical axis in nematic phases. The sample and PEM were placed between crossed linear polarizers, with axes rotated ±45 deg with respect to the PEM axis, and the intensity of the light transmitted through this set-up was measured with a photodiode (FLC Electronics PIN-20). The registered signal was de-convoluted with a lock-in amplifier (EG&G 7265) into 1f and 2f components to yield a retardation induced by the sample. Based on the measured optical birefringence the conical tilt angle (θ) in the twist-bend ferroelectric nematic phase (N_{TBF}) was deduced from the decrease of the Δn with respect to the values measured in the ferroelectric nematic (N_F) phase, according to the relation: $\Delta n_{NTBF} = \Delta n_{NF} (3 \cos^2 \theta - 1)/2$ [17]. The birefringence of the ferroelectric nematic phase was extrapolated to the lower temperature range by assuming a power law temperature dependence: $\Delta n_{NF} = \Delta n_0 (Tc - T)^{\gamma}$, where Δn_0, Tc , and γ are the fitting parameters.

Laser diffraction studies: Optical diffraction studies were performed for the samples placed on a heating stage and illuminated from below with green (520 nm) laser light. The diffraction pattern was

recorded on the half-sphere screen placed above the sample, the angular position of the observed diffraction signal allowed for calculation of the related periodicity of the stripe pattern in the cell, and helical pitch length.

Dielectric spectroscopy: The complex dielectric permittivity was measured in the 1 Hz–10 MHz frequency range using a Solartron 1260 impedance analyzer. The material was placed in 3-μmthick glass cell with ITO electrodes (without the polymer alignment layers to avoid the influence of the high capacitance of a thin polymer layer). The amplitude of the applied ac voltage, 20 mV, was low enough to avoid Fréedericksz transition in nematic phases.

Atomic Force microscopy (AFM) and Piezoresponse Force Microscopy (PFM):

AFM measurements were performed using a Bruker Dimension Icon Microscope working in tapping or Peak Force Quantitative Nanomechanics (QNM) mode and cantilevers with 0.4 N/m force constant were applied. The PFM experiments were conducted with the same instrument, in an optimized vertical domains mode. In this setup, the deflection of a conducting AFM cantilever is detected as the piezoelectric material's domains deform mechanically in response to an applied voltage. Due to the small magnitude of these displacements, a lock-in technique is used. A modulated reference voltage is applied to the AFM tip, inducing deformation of the sample surface. The AFM tip remains in contact mode during the measurement. The lock-in amplifier detects the cantilever's deflection signal, which oscillates in phase with the reference drive signal during deformation, and out of phase (perpendicular) when no deformation occurs. These signals are then converted into amplitude and phase angle data for the cantilever deflection. Ideally, at the domain wall, the amplitude should drop to zero, and the phase should shift by 180 degrees.

The sample was placed on an ITO electrode surface, which was electrically connected to the AFM stage. The PFM measurements were performed with dedicated to soft material use Budget Sensors AIOE cantilevers with a resonance frequency of 15 kHz and a 0.2 N/m force constant.

Organic synthesis and analytical data:

Studied here material, 4'-(difluoro(3,4,5-trifluorophenoxy)methyl)-2,3'-difluoro-[1,1'-biphenyl]-4-yl 2,6-difluoro-4-(5-propyl-1,3-dioxan-2-yl)benzoate was synthesized at Liquid Crystal group of the Military University of Technology is modification of JK103 structure [1]. In first step , 2,6-difluoro-4-(5-propyl-1,3-dioxan-2-yl)benzoic acid **(3)** was synthesized following the procedure in [2].

In order to purify the **(3)** to a pure *trans* form of 1,3-dioxane unit, a series of recrystallization processes were performed, after which the compound was constantly enriched with the *trans* isomer. The recrystallisation process was repeated until > 99% isomeric purity was achieved.

Next, during the Suzuki-Miyaura process the phenol derivative **(3)** was obtained by reacting boronic pinacol ester derivative **(2)**, obtained previously from bromo derivative **(1)** in a Miyaura borylation reaction, with the 4-bromo-3-fluorophenol. Final compound was synthesized in a Steglich

esterification conditions between **(3)** and **(4)** with the presence of DCC and DMAP. The compound was purified using sequence of recrystallization and liquid column chromatography techniques.

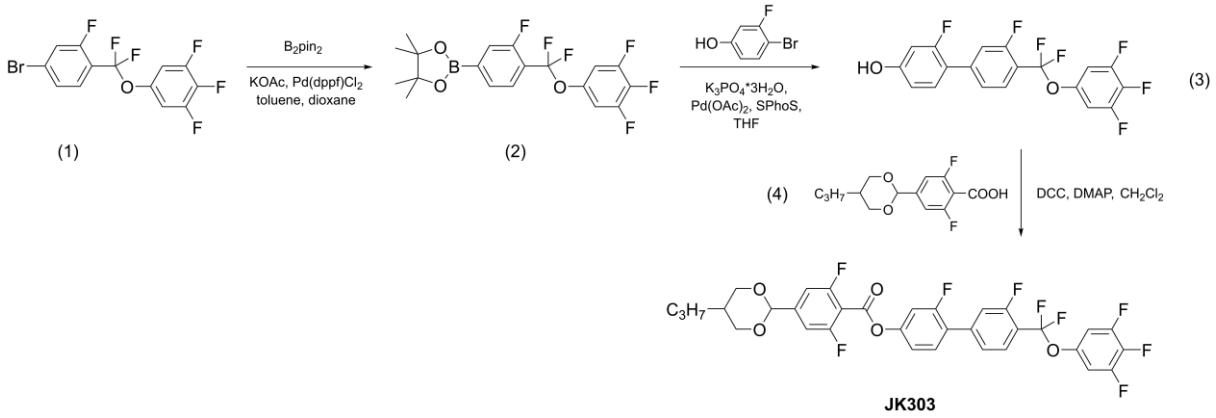

Fig. S1. Synthesis of studied compound 4'-(difluoro(3,4,5-trifluorophenoxy)methyl)-2,3'-difluoro-[1,1'-biphenyl]-4-yl 2,6-difluoro-4-(5-propyl-1,3-dioxan-2-yl)benzoate

2-(4-(difluoro(3,4,5-trifluorophenoxy)methyl)-3-fluorophenyl)-4,4,5,5-tetramethyl-1,3,2,-dioxaborolane (2)

5-((4-bromo-2-fluorophenyl)difluoromethoxy)-1, 2,3-trifluorobenzene **(1)** (6.6 g - 0.018 mol), bis(pinacolato)diboron (4.8 g - 0.019 mol), potassium acetate (5.29 g - 0.054 mol), toluene and dioxane (1:1 vol/vol) were placed in flask. The reaction was refluxed under a nitrogen atmosphere. $PdCl_2$(dppf) (0.4 g - 0.00054 mol) was then added. The reaction was refluxed for 48 h under a nitrogen atmosphere. The reaction was poured into water and filtered under reduced pressure through a Fuller's earth plate. The phases were separated by washing the organic phase with water and the aqueous phase with toluene. The organic phase was dried over anhydrous $MgSO_4$ and concentrated. Product was purified using chromatography column (silica gel, hexane).

Yield 5.2 g (70%).
Purity 95% (GC-MS)
m.p. = 55-57°C
MS(EI) m/z: 418 (M+); 403; 319; 255; 241; 229; 213; 189; 171; 144; 131; 119

^{1}H NMR (500 MHz, $CDCl_3$) δ: 7.67 (m, 2 H); 7.61 (d, *J*=10.99 Hz, 1 H); 6.98 (t, J=6.85 Hz, 2H); 1.38 (s, 12 H)

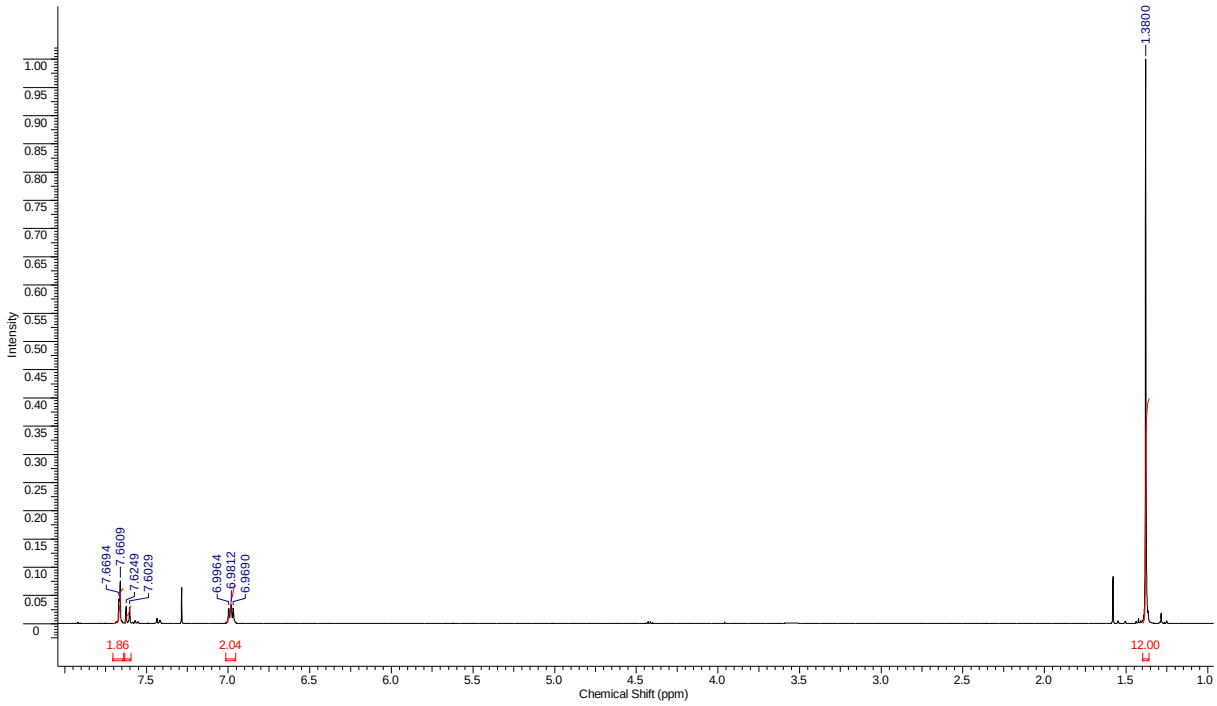

^{13}C NMR (125 MHz, $CDCl_3$) δ: 158.38; 152.00 (dd, *J*=10.90, 5.45 Hz); 150.00 (dd, J= 10.83, 5.45 Hz); 144.96 (m); 139.33 (t, *J*=14.99 Hz); 137.34 (t, *J*=15.44 Hz); 130.07 (d, *J*=3.63 Hz); 126.73 (t, *J*=5.00 Hz); 122.56 (m); 122.40; 120.79; 107.41 (m); 84.57; 24.87

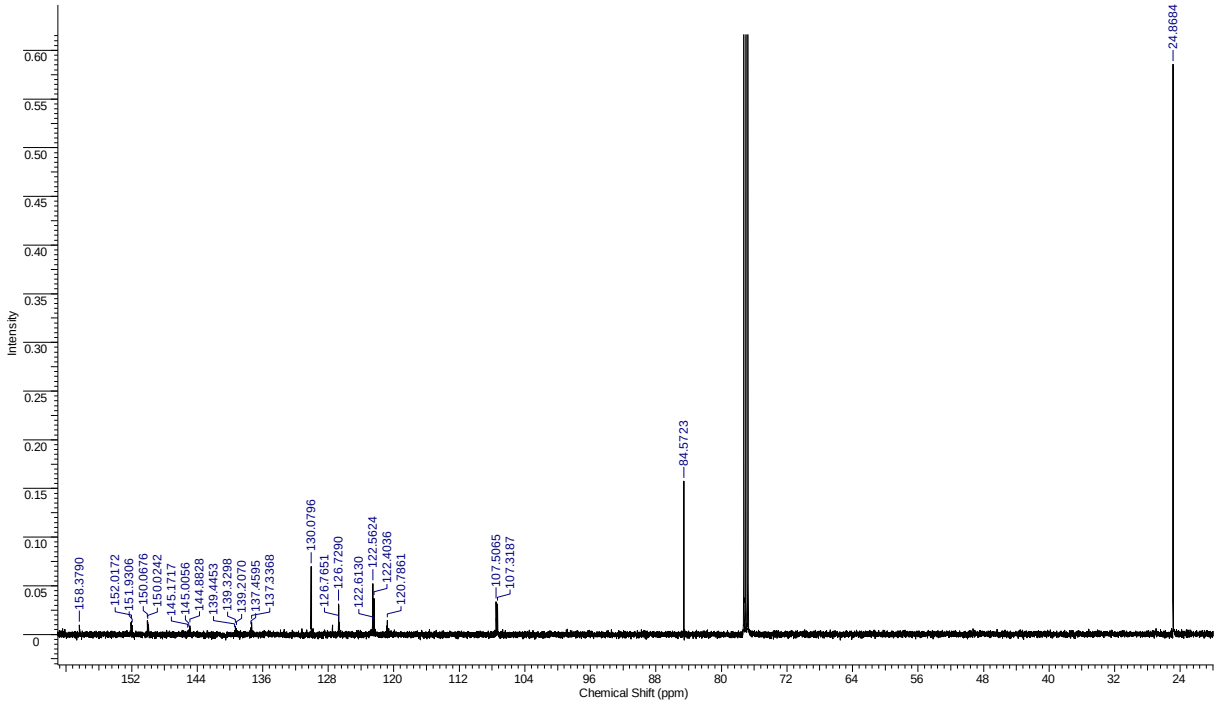

4'-(difluoro(3,4,5-trifluorophenoxy)methyl)-2,3'-difluoro-[1,1'-biphenyl]-4-ol (3)

2-(4-(difluoro(3,4,5-trifluorophenoxy)methyl)-3-fluorophenyl)-4,4,5, 5-tetramethyl-1,3,2,-dioxaborolate **(2)** (3.7 g - 0.009 mol), 4-bromo-3-fluorophenol (1.54 g - 0.008 mol), K_3PO_4 * $3H_2O$ (8.4 g - 0.031 mol) and 250 cm^3 of anhydrous tetrahydrofuran were placed in flask. The reaction was refluxed under a nitrogen atmosphere. $Pd(OAc)_2$ (0.047 g - 0.00022 mol) and SPhos (0.092 g - 0.00022 mol) were then added. The reaction was refluxed for 24 h under a nitrogen atmosphere. Reaction was washed with water and dichloromethane; filtered off; product was extracted with dichloromethane; the organic layer was washed with water, dried over anhydrous $MgSO_4$ and concentrated. Phenol was concentrated and purified using chromatography column (silica gel, dichloromethane).

Yield 1.5 g (47%).
Purity 92% (GC-MS)
m.p. = 94-96°C
MS(EI) m/z: 402 (M+); 383; 331; 297; 255; 235; 226; 206; 186; 175; 157; 147; 119

^{1}H NMR (500 MHz, $CDCl_3$) δ: 7.72 (t, *J*=7.93 Hz, 1 H); 7.36 (m, 3 H); 7.01 (dd, *J*=7.63, 6.10 Hz, 2 H); 6.74 (m, 2 H)

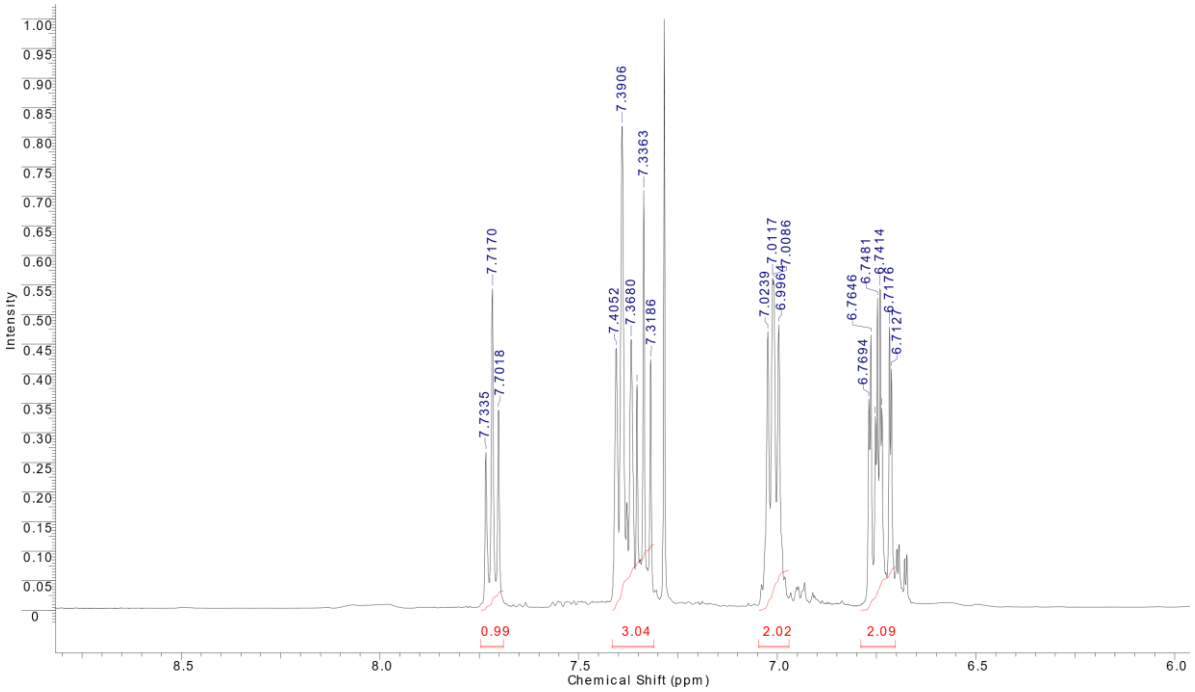

^{13}C NMR (125 MHz, $CDCl_3$) δ: 162.29; 159.31; 157.54 (d, *J*=11.8 Hz); 150.99 (dd, *J*=250.3, 16.3 Hz); 131.04; 127.30; 124.04; 118.96 (t, *J*=10.0 Hz); 116.98 (d, *J*=18.2 Hz); 107.51 (d, *J*=21.8 Hz); 104.02 (d, *J*=26.3 Hz)

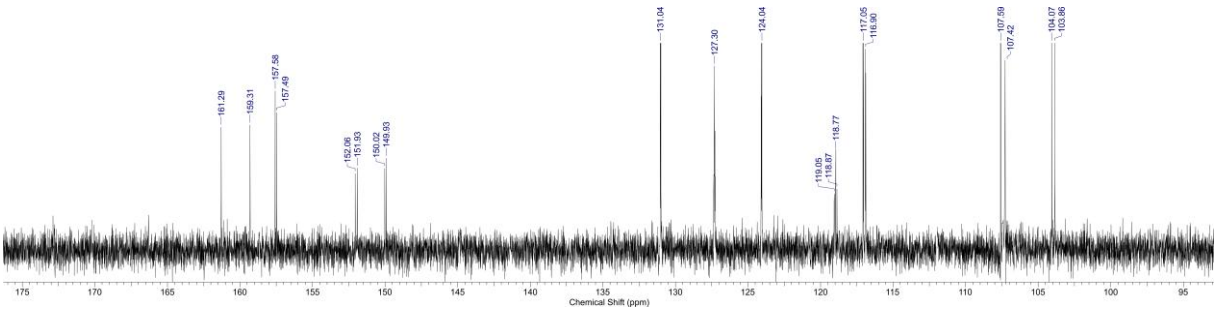

4'-(difluoro(3,4,5-trifluorophenoxy)methyl)-2,3'-difluoro-[1,1'-biphenyl]-4-yl 2,6-difluoro-4-(5-propyl-1,3-dioxan-2-yl)benzoate

To a stirred solution of 2,6-difluoro-4-(5-propyl-1,3-dioxan-2-yl)benzoic acid **(4)** (1.0 g; 0.003 mol), 4'-(difluoro(3,4,5-trifluorophenoxy)methyl)-2,3'-difluoro-[1,1'-biphenyl]-4-ol **(3)** (1.5 g; 0.0037 mol) and N,N'-dicyclohexylcarbodiimide DCC (0.8 g; 0.004 mol) in dichloromethane, DMAP (0.1g) was added and the solution was stirred overnight at room temperature. The reaction mixture was filtered through silica pad and the filtrate was concentrated under vacuum. The product was purified using sequence of recrystallization (ethanol/acetone mixture) and liquid column chromatography (silica gel and dichloromethane) techniques to give white solid.

Yield 0.9g (36%)
Purity 99.5% (99.6/0.2 trans/cis ratio) (HPLC-MS)
MS(EI) m/z: 670 (M+); 652; 523; 423; 401; 369; 269; 254; 226; 206; 185; 169; 141

^{1}H NMR (500 MHz, $CDCl_3$) δ: 7.77 (t, *J*=7.93 Hz, 1 H); 7.52 (t, *J*=8.70 Hz, 1 H); 7.44 (m, 2 H); 7.21 (m, 4 H); 7.02 (dd, *J*=7.63, 5.80 Hz, 2 H); 5.43 (s, 1 H); 4.28 (dd, *J*=11.75, 4.73 Hz, 2 H); 3.56 (t, *J*=11.44 Hz, 2 H); 2.16 (m, 1 H); 1.37 (m, 2 H); 1.13 (m, 2 H); 0.96 (t, *J*=7.32 Hz, 3 H)

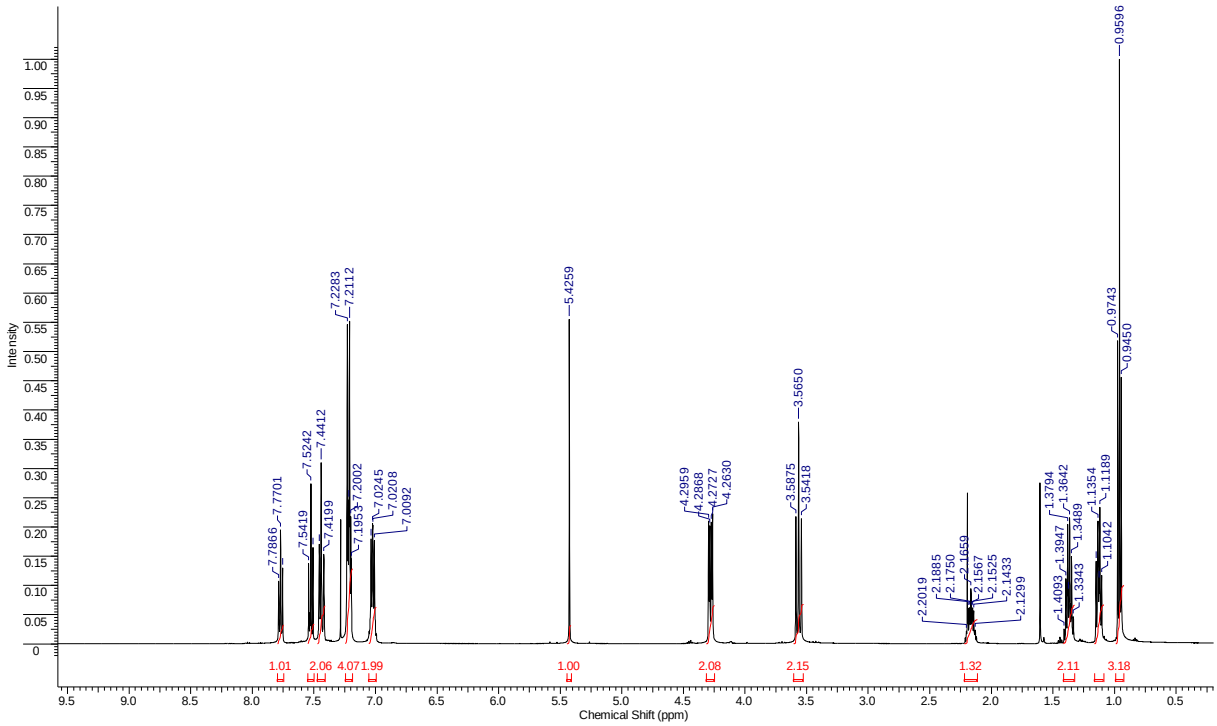

^{13}C NMR (125 MHz, $CDCl_3$) δ: 161.97 (d, *J*=5.45 Hz); 160.75; 160.55; 159.92 (d, *J*=5.45 Hz); 159.28; 158.71; 158.55; 152.04 (dd, *J*=10.90, 5.45 Hz); 151.23 (d, *J*=10.90 Hz); 150.04 (dd, *J*=10.90, 5.45 Hz); 145.68 (t, *J*=9.99 Hz); 144.87 (m); 140.58 (d, *J*=8.17 Hz); 139.37 (t, *J*=15.44 Hz); 137.39 (t, *J*=15.44 Hz); 130.87 (d, *J*=3.63 Hz); 127.54 (m); 124.75 (dd, *J*=13.62, 1.82 Hz); 124.47 (t, *J*=3.18 Hz); 120.74 (t, J=264,31 Hz); 119.73 (m); 118.16 (d, *J*=3.63 Hz); 117.41 (dd, *J*=22.71, 3.63 Hz); 110.66 (d, *J*=25.43 Hz); 110.32 (dd, *J*=23.16, 3.18 Hz); 109.46 (t, *J*=17.26 Hz); 107.43 (m); 98.82; 72.60; 33.92; 30.25; 19.55; 14.18

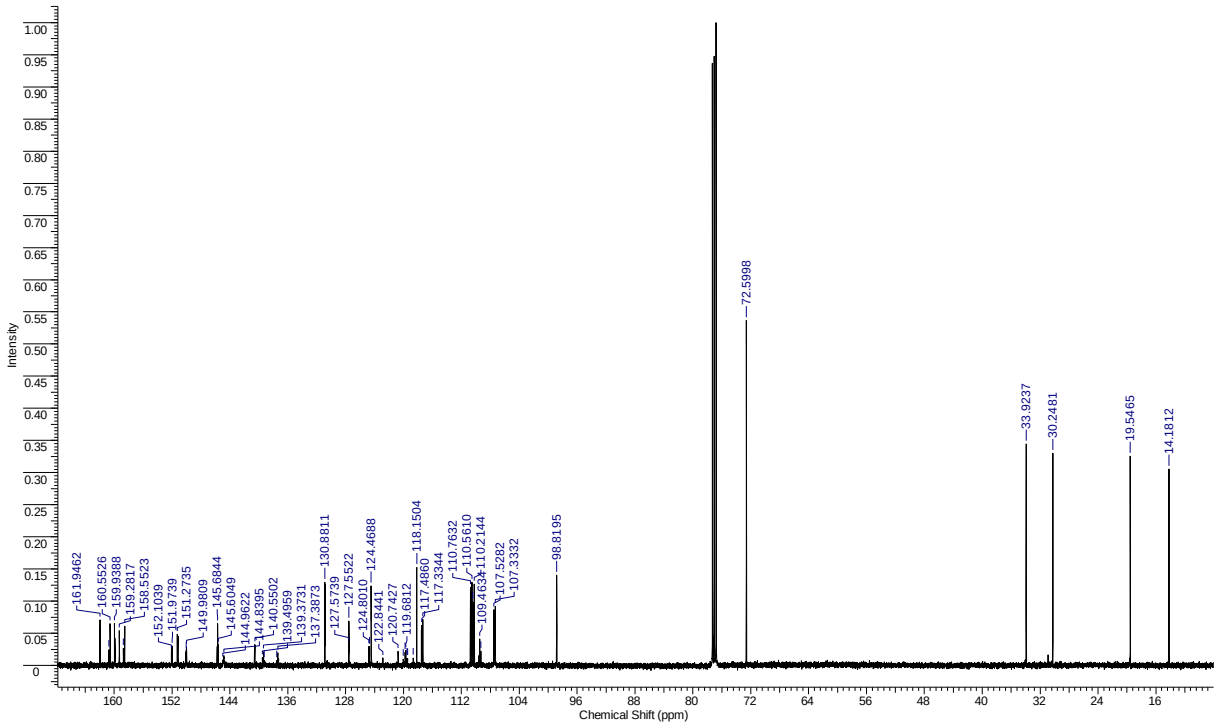

Suplementarny results

Table 1. Phase transition temperatures (°C) and associated thermal effects (kJ/mol)

heating	Cr 71.0 (23.61) N_F 118.0 (0.005) N_X 119.8 (0.12) N 250.6 (1.12) Iso
cooling	Iso 237.0 (1.0) N 118.9 (0.085) N_X 114.3 (0.005) N_F 59.0[a] N_{TBF} 55.4 (0.22) SmC_P^H 6.6 (7.26) Cr

[a] from microscopic observations

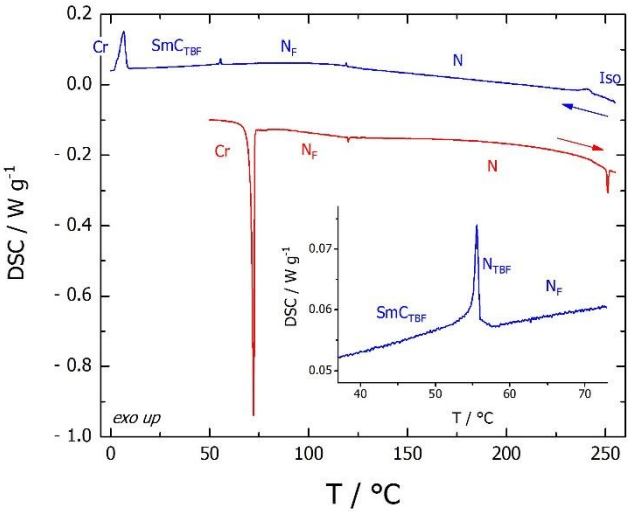

Figure S1. DSC thermograms for heating (red line) and cooling (blue line) scans. In the inset: enlarged temperature range near N_F-N_{TBF}- SmC_P^H phase transitions

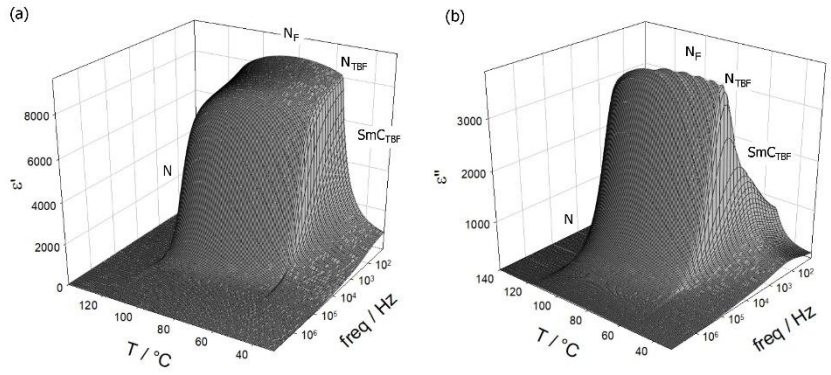

Figure S2. Real (a) and imaginary (b) part of dielectric permittivity vs. temeprature and frequency. Measured complex impedance of the tested cell filled with LC material has been analyzed assuming equivalent circiuit of capacitor and resistor in parallel connection to yield the components of permittivity.

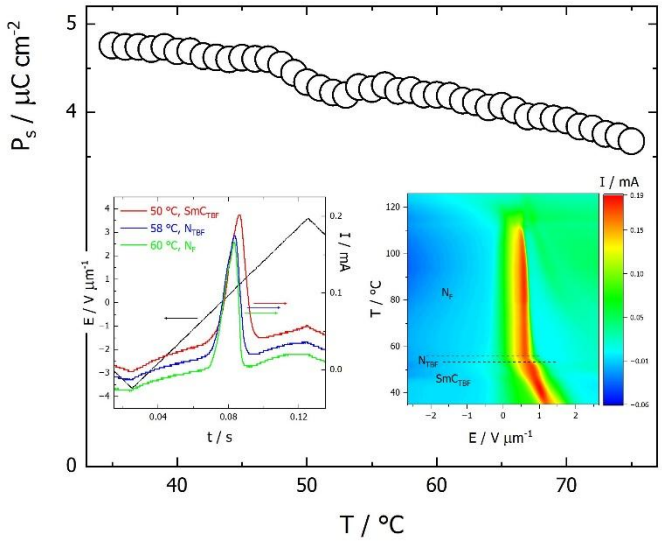

Figure S3. Spontaneous electric polarization vs. temperature, determined by integration of the switching current after subtracting linear background due to finite ohmic resistivity (ionic conductivity). In the left inset: switching current in SmC_P^H, N_{TBF} and N_F phases (red, blue, green lines, respectively) recorded under application of triangular-wave voltage (black line). In the right inset: position of the switching current peak vs. applied electric field and temperature. In SmC_P^H phase the threshold voltage (current peak position) for the switching of polarization considerably increases.

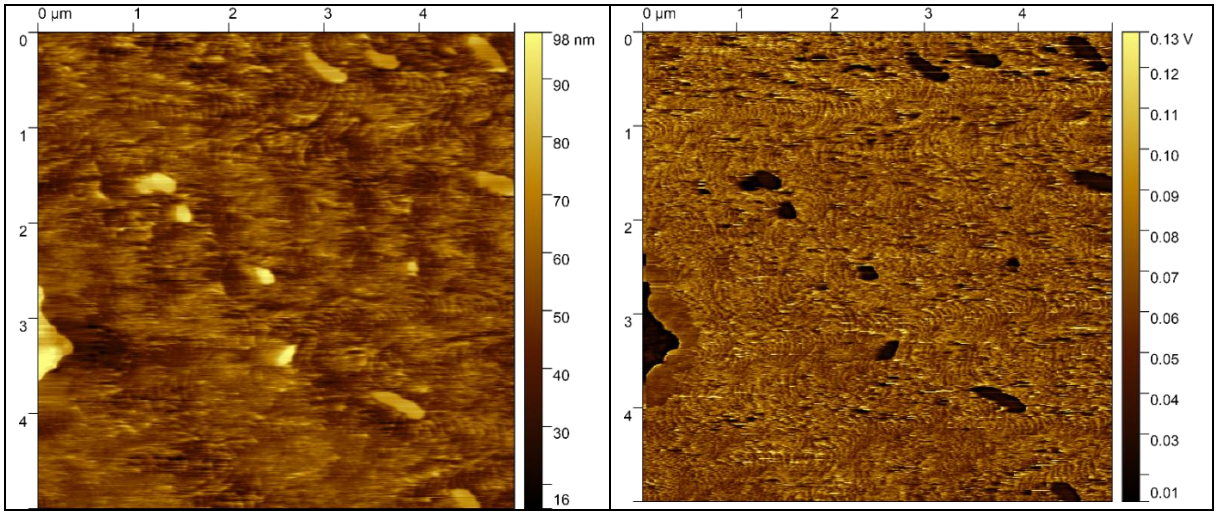

Figure S4. AFM image revealing the sub-micrometer structure in the SmC_P^H phase: (left) Height and (right) adhesion modes. The weak wavy patterns are most probably the Bouligand arches [3] related to the heliconical structure of the phase.

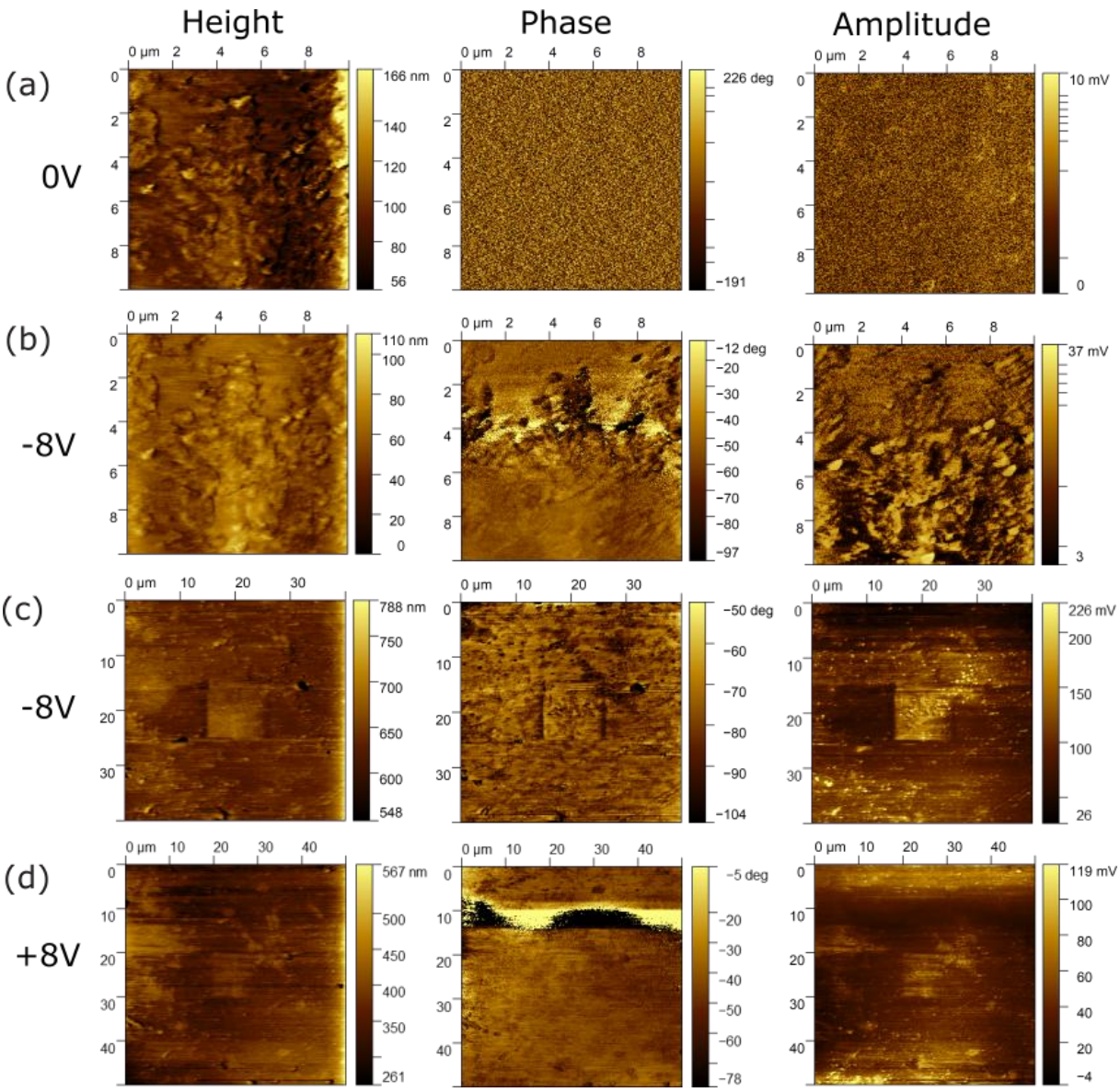

Figure S5. (a) 10 x 10 µm sample area measured before application of bias electric field. (b) The same area observed under applied bias voltage (-8V). The measurement under applied bias causes the reorientation of ferroelectric domains. (c) With the -8V bias still applied, measurements were taken over a 40 x 40 µm area. The pre-treated 10 µm square area was clearly visible in the center of the sample. (d) Reversing of the bias voltage to +8V caused the polarization within the 10 µm square domain to be nearly erased. While some remnants of the original domain were still visible in the topography (Height mode), the phase and amplitude were almost completely rewritten.

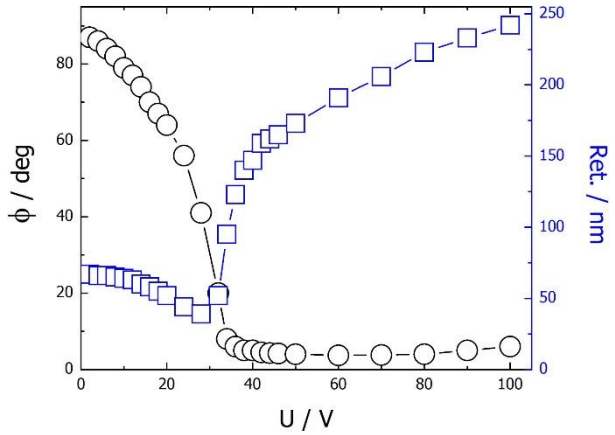

Figure S6. Relative orientation of optical axis (ϕ, black circles) and optical retardation (Ret., blue squares) vs. applied voltage measured in SmC_P^H phase. A 2.5-μm-thick cell with parallel electrodes on one substrate was used allowing for application of in-plane electric field. The cell surfaces were treated for planar anchoring and were rubbed in direction perpendicular to the electric field.

Movie S1. Changes of the laser light diffraction patterns observed on spherical screen in SmC_P^H phase (2.5-μm-thick cell with in-plane electrodes, planar anchoring and rubbing direction perpendicular to the electric field) under applied triangular-wave voltage (0.1Hz, 160 V_{pp}). Above a certain threshold only diffraction spots positioned along the applied electric field are visible (vertical direction on the movie). When applied electric field is below threshold additional set of diffraction spots appear, along the rubbing direction (horizontal direction on the movie).

References

1. J. Karcz, J. Herman, N. Rychłowicz, P. Kula, E. Górecka, J. Szydlowska, P. W. Majewski, D. Pociecha, *Science* 2024, **384**, 1096–1099.
2. J. Karcz, N. Rychłowicz, M. Czarnecka, A. Kocot, J. Herman, P. Kula, *Chem. Commun.* 2023, **59**, 14807-14810
3. Y. Bouligand, M.-O. Soyer, S. Puiseux-Dao, *Chromosoma*, 1968, **24**, 251–287